

# Tandem-L: Design Concepts for a Next-Generation Spaceborne SAR System

Sigurd Huber, German Aerospace Center (DLR), Germany, sigurd.huber@dlr.de

Michelangelo Villano, German Aerospace Center (DLR), Germany

Marwan Younis, German Aerospace Center (DLR), Germany

Gerhard Krieger, German Aerospace Center (DLR), Germany

Alberto Moreira, German Aerospace Center (DLR), Germany

Bernhard Grafmüller, Airbus Defense & Space, Germany

Reinhard Wolters, Airbus Defense & Space, Germany

## Abstract

Tandem-L is a fully polarimetric bistatic spaceborne SAR mission with the goal of monitoring dynamic processes on the Earth's surface. Important applications are regular inventories of the global-scale biomass, systematic measurements of surface deformations with millimeter accuracy, the generation of digital surface and terrain models, as well as disaster monitoring related to flooding events, earthquakes and volcano eruptions. To serve this wide variety of services and applications, the imaging and mapping requirements exceed those of state-of-the-art missions by at least one order of magnitude.

Such a pioneering mission necessarily initiates new technology developments in the fields of radar hardware, data processing and data distribution. The Tandem-L radar satellites employ large unfoldable mesh reflector antennas, which have been identified ideal for highly sensitive, high-resolution wide-swath SAR acquisitions. This paper gives an overview of the system concepts of next-generation SAR sensors like Tandem-L and details some of the design aspects and optimisation potentials leading to an improved performance and fulfilling the user requirements.

## 1 Introduction

Nearing the end of a Phase A study the Tandem-L mission concept has reached a mature status [5, 6]. The mapping capability of the Tandem-L satellites will exceed those of present day SAR sensors by almost two orders of magnitude, allowing for global coverage twice a week. The SAR sensors have to reflect these demanding user requirements in terms of a sophisticated design, with the driving parameters summarized in **Table 1**.

mode	1	2	3
polarization	single	dual	quad
bandwidth	80 MHz	80 MHz	80 MHz
azimuth res.	7 m	7 m	7 m
swath width	350 km	350 km	175 km
<i>NE SZ</i>	< -25 dB	< -25 dB	< -28 dB
<i>ASR</i>	< -25 dB	< -25 dB	< -22 dB

**Table 1:** Main Tandem-L imaging modes. The ambiguity-to-signal ratio *ASR* accounts for range and azimuth ambiguities.

Tandem-L shall map the Earth surface in an 745 km orbit with incident angles greater than  $26.3^\circ$  at L-band frequencies centered around 1.2575 GHz. It turned out that, at a reasonable cost-value ratio, only a reflector antenna based concept can serve the requirements of a sensitivity better than  $-25$  dB at swath widths of up to 350 km. Representing the state-of-the-art in communications, array-fed reflector antennas have found their way into upcom-

ing SAR missions like BIOMASS [1], NISAR [7, 10] and Tandem-L. What makes these antennas attractive for radar applications is the fact that large apertures can be installed in space using light-weight mesh structures, for instance composed of carbon fibre reinforced silicone (CFRS). The feed array resembles an active phased array antenna, common for many SAR sensors. New in this context is that the SAR signal is digitized almost immediately after reception. This offers the opportunity to employ new SAR imaging modes and to flexibly adapt the associated beamforming schemes, e.g. to varying topography.

## 2 Reflector SAR Operation

The operation principle of an array-fed reflector SAR system is illustrated in **Figure 1**. The reflector is illuminated by an array of feed elements, which are typically patch antennas at L-band frequencies. On transmit all elements are activated simultaneously such that the entire swath is covered by a wide and broad antenna footprint. In contrast to direct radiating arrays, in the reflector case each feed element illuminates a distinct spot in this footprint. This means there is basically a direct mapping between the feed array topology and the Earth surface. On receive, a couple of elements are used in each elevation column to trace the emitted radar echo on ground employing digital beamforming (DBF) techniques [4, 11, 2, 3]. After this elevation beamforming, the associated signals are then downlinked for further processing on ground.

A further innovation to be realized onboard the Tandem-L satellites is the so called staggered pulse scheme [8]. The key idea is to vary the pulse repetition interval (PRI) from pulse to pulse in such a way that never two consecutive pulses are lost for a given range. By this it is possible to avoid the typical blind ranges dictated by the timing constraints of conventional fixed-PRI SAR systems.

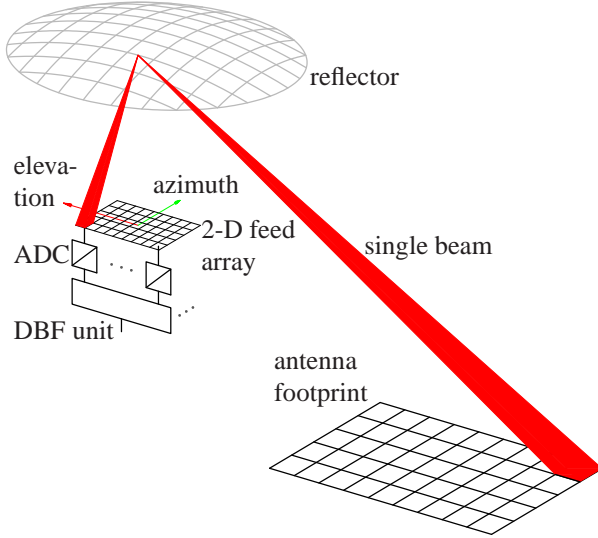


**Figure 1:** Array-fed reflector principle. Each cell in the antenna footprint is associated with an element in the 2-D feed array. On transmit a wide and broad beam is generated by simultaneously activating all feed elements. On receive a high gain beam follows the pulse echo on ground using the elements in a specific elevation column. These elevation column signals are downlinked for further azimuth processing on ground.

### 3 The Tandem-L SAR Antenna

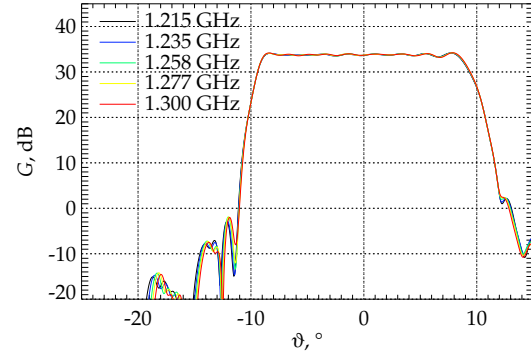
In view of the challenging imaging requirements of Tandem-L, a large array-fed reflector antenna has been considered as best solution. The most important geometrical dimensions are listed in **Table 2**. The projected circular aperture of the parabolic reflector has a diameter of 15 m resulting in a maximum theoretical directivity of 45.9 dB. In order to minimize multipath effects between the reflector and the feed array a relatively large offset in elevation of 9 m has been chosen.

diameter	15 m
focal length	13.5 m
offset (elevation)	9 m
azimuth elements	6
elevation elements	32
azimuth spacing	$0.6 \lambda$
elevation spacing	$0.6816 \lambda$

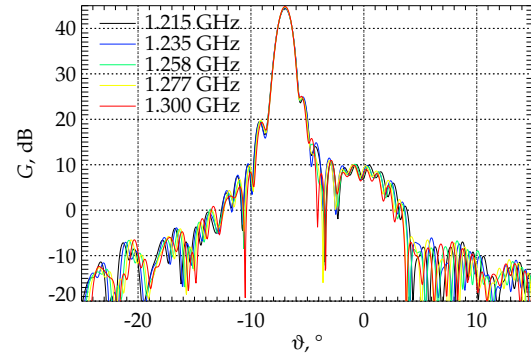
**Table 2:** Tandem-L reflector and feed array specification.

**Figure 2a** shows an elevation cut of the transmit patterns at five frequency points within the 85 MHz band.

In **Figure 2b** an example of a receive beam after elevation beamforming is shown. Both plots suggest that the patterns can be expected to vary mildly over frequency within the main beam region. This is clearly a consequence of the large offset.



(a)



(b)

**Figure 2:** (a) Transmit pattern versus elevation angle at five discrete frequency points. (b) Example of a receive beam pointing at near range.

As schematically indicated in **Figure 3** the planar feed array is composed of 32 microstrip patch elements in elevation and six elements in azimuth. A peculiarity of this design is that always two feed elements are combined to a doublet in such a way that cross-polar field components are damped. This results in three azimuth rows of 32 feed doublets. Finally, always three azimuth doublets are pre-summed using fixed weights and thereby form a single digital elevation channel. This is motivated by the fact that the staggered SAR scheme requires a relatively large pulse repetition frequency (PRF) raising the need of optimized azimuth beams in order to mitigate azimuth ambiguities. The fixed complex coefficients  $w_{ij}$  apply on transmit as well as on receive. A potential implementation of this concept might be by means of power dividers/combiners and different cable lengths for phase adjustment. After reception and digitization the individual elevation signals are combined to a single data stream in the DBF unit.

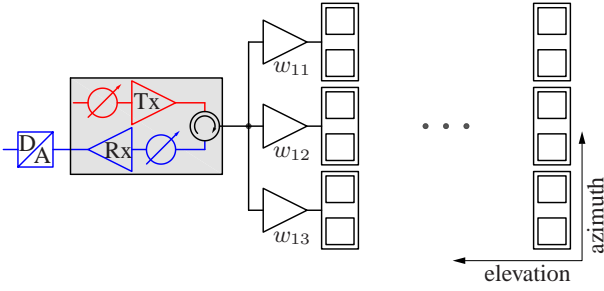


**Figure 3:** Basic hardware architecture of the feed array. The fixed complex weights  $w_{ij}$  shall be realized via different cable lengths and power dividers/combiners.

## 4 Data Volume Reduction

In order to meet typical azimuth ambiguity requirements, a staggered SAR system needs to employ a high mean  $PRF$  on transmit, i.e., data are to be oversampled in azimuth. This causes an increased data volume, which can be, however, reduced by on-board Doppler filtering and decimation [9]. This data volume reduction strategy can be better understood considering first the case of a SAR system with constant  $PRI$ . If data were just decimated prior to downlink (e.g., by a factor of 2 if the  $PRF$  is larger than twice the processed Doppler bandwidth), a considerable degradation of the  $AASR$  would occur. However, if Doppler filtering is performed before decimation, the additional ambiguous energy due to decimation can be substantially reduced. Due to the large amount of data, acquired by typical high-resolution wide-swath (HRWS) systems, the number of on-board operations per sample has to be minimized, while avoiding a degradation of the impulse response. The Doppler filtering can be therefore performed in time domain using a finite impulse response (FIR) filter with a relatively small number of taps. The filter will introduce a distortion of the Doppler spectrum of the signal, which can be compensated for in the SAR processing (on ground). In a staggered SAR system, the Doppler filter has to be applied to raw data resampled to a uniform  $PRI$ , but, in practice, resampling, Doppler filtering, and decimation can be also jointly performed. Each sample of the resampled data is obtained as a linear combination of some of the samples of the raw staggered SAR data, while each sample of the filtered data is obtained as a linear combination of some of the resampled data. This means that each sample of the filtered data can be obtained directly as a linear combination of some of the staggered SAR data. Moreover, there is no need to compute the samples, which would anyway be discarded by the decimation operation. The FIR filter can be designed as a Wiener filter, i.e., exploiting the knowledge of the power spectral density (PSD) of the useful and disturbance signals. An alternative to design the FIR Wiener filter is given by the minimum variance distortion less response (MVDR) or Capon beamformer, where only the knowledge of the PSD of the disturbance signal is exploited. The formulas for the de-

sign of the filter and the consequent  $AASR$  degradation are provided in [9].

## 5 Staggered SAR Performance

The Tandem-L SAR instruments support fully polarimetric operation. In the subsequent performance analysis it is assumed that the power of the TRMs of both polarization channels can be routed to a single polarization channel, effectively doubling the output power. Each TRM has an output power of 56.6 W. Alternatively, TRMs with twice the output power might be regarded during later phases. As mentioned above a relatively high mean  $PRF$  is required for acceptable azimuth ambiguity levels, which lie at 2600 Hz for the single- and dual-pol modes and at  $2 \times 2100$  Hz for the quad-pol mode. The respective pulse duty cycles are chosen to be 4% and 8% resulting in quite short pulses. These pulses can be tracked by the Tandem-L beams without significant losses, since the beams are broader than the projected pulse extension. Nevertheless, the pulse duty cycle offers some margin for adjustment in case more transmit power might be needed. **Figure 4** summarizes the performance in single-/dual and quad-pol operation. As beamforming technique in elevation MVDR beamforming on receive [3] has been used to maximize the sensitivity.

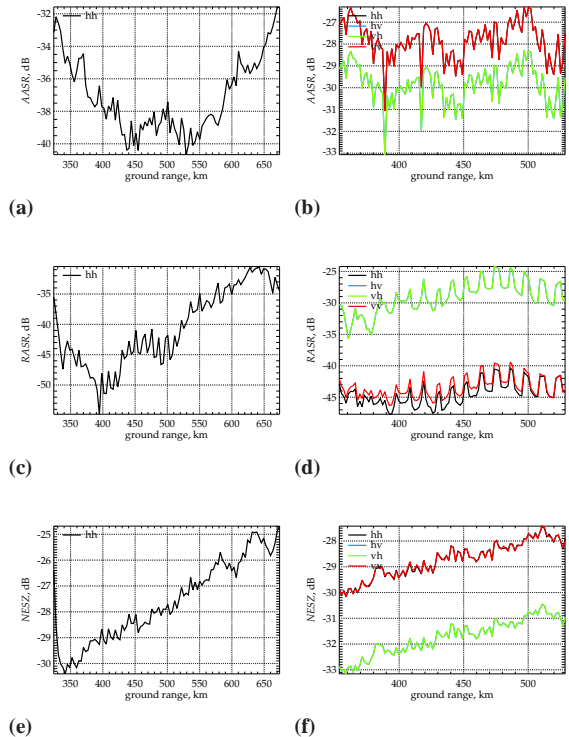


**Figure 4:** Azimuth ambiguity-to-signal ratio ( $AASR$ ) for single-pol mode (a) and for quad-pol mode (b). Range ambiguity-to-signal ratio ( $RASR$ ) for single-pol mode (c) and for quad-pol mode (d). Noise equivalent sigma zero ( $NESZ$ ) for single-pol mode (e) and for quad-pol mode (f).

Especially the quad-pol mode with its high average  $PRF$  turned out to be a design driver. Therefore, the swath width had to be halved to 175 km in order to meet the performance requirements. The quad-pol performance proved to be best with the swath starting at an incident angle of  $28.4^\circ$ , closer to near range. Additionally, a concept has been exploited where the cross-polarized channels have been merged. By this the cross-polar  $AASR$  could be improved in the order of 2 dB, while the cross-polar  $RASR$  and  $NESZ$  benefit by a factor of two.

## 6 A High-Resolution Mode

So far Tandem-L is intended to acquire SAR imagery with resolutions down to 7 m. Due to potential demands of finer azimuth resolutions in the future also the concept of a 3-m mode has been investigated. In principle the feed design discussed above is capable of covering the required Doppler frequency domain. This can be realized by recording and downlinking the three azimuth rows separately and applying multi azimuth channel processing techniques [3]. However, it showed that the performance degrades severely in near and in far range due to defocusing effects. This motivated an optimization of the feed array from the scratch. For this, plane waves, originating from within the desired antenna footprint, have been simulated. These plane waves generate, after deflection at the reflector, an electromagnetic field in the plane of the feed array. Then, feed elements have been placed such that at least 80 % of the power of the incident plane wave is captured. Repeating this process for each plane wave from within the antenna footprint finally gives the entire feed array as depicted in **Figure 5**. This feed design shows a distinct 'bone' shape, which can be explained due to the defocused fields especially in far range (left part of the plot). Please note, that the patch elements are quadratic and only appear rectangular due to the different scales of the axes.

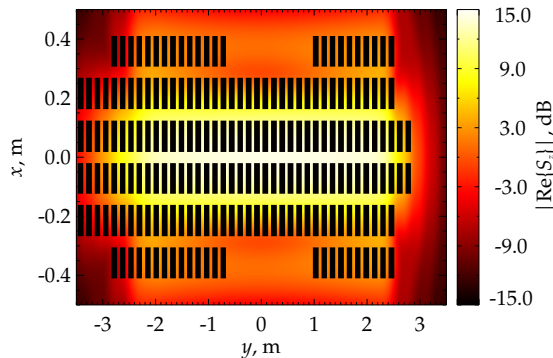


**Figure 5:** Field distribution in the feed array plane. The patch elements are placed such that, for each incident plane wave, more than 80 % of the incident power is collected.

For the purpose of performance computation the 'bone' shaped feed array has been filled up to a rectangular

shaped array with three individual azimuth channels. **Figure 6** shows the stripmap performance (i.e. constant PRI with range gaps) for the single-/dual-pol modes with a  $PRF$  of 2600 Hz and for the quad-pol modes at a  $PRF$  of  $2 \times 2330$  Hz. It is important to mention that only the very basic MVDR beamformer has been applied here and no nullsteering concepts. The goal here was clearly to have a design which is inherently robust. The ambiguity performance for the quad-pol mode is only violated punctually, but this might be mitigated to a certain degree by more sophisticated beamforming techniques. Also noteworthy is that the quad-pol mode shows an excellent sensitivity. This is because here the 175 km swath is acquired using the near range beams.

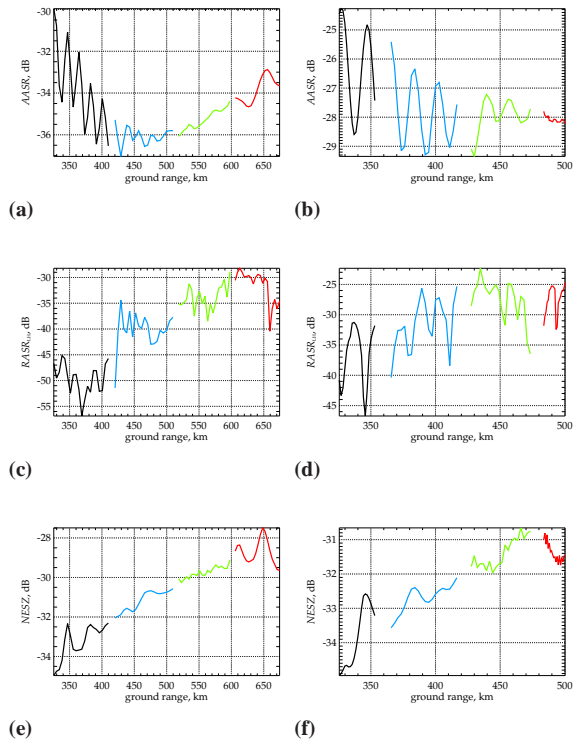


**Figure 6:** Performance for the 3-m stripmap mode with constant PRI (gaps). Azimuth ambiguity-to-signal ratio ( $AASR$ ) for single- and dual-pol modes (a) and for quad-pol mode (b). Range ambiguity-to-signal ratio ( $RASR$ ) for single- and dual-pol modes (c) and for quad-pol mode (d). Noise equivalent sigma zero ( $NESZ$ ) for single- and dual-pol modes (e) and for quad-pol mode (f).

## 7 Conclusion

Tandem-L is an interferometric spaceborne SAR mission with ambitious goals. In this paper some ideas and concepts have been presented which help to realize such a next-generation SAR system. It has been shown, that the performance requirements can be met employing an innovative digital feed array. Beyond that a way to implement a high-resolution mode with multiple azimuth channels has been discussed.

## References

- [1] M. Arcioni, P. Bensi, M. Fehringer, F. Fois, F. Hellere, C.-C. Lin, and K. Scipal, "The Biomass Mission, Status of the Satellite System," in *IEEE International Geoscience and Remote Sensing Symposium (IGARSS)*, Jul 2014, pp. 1413–1416.
- [2] A. Freeman, G. Krieger, P. Rosen, M. Younis, W. Johnson, S. Huber, R. Jordan, and A. Moreira, "SweepSAR: Beam-forming on Receive using a Reflector-Phased Array Feed Combination for Spaceborne SAR," in *IEEE Radar Conference (RadarCon)*, May 2009.
- [3] S. Huber, M. Younis, A. Patyuchenko, G. Krieger, and A. Moreira, "Spaceborne Reflector SAR Systems with Digital Beamforming," *IEEE Transactions on Aerospace and Electronic Systems*, vol. 48, no. 4, pp. 3473–3493, Oct 2012.
- [4] G. Krieger, N. Gebert, M. Younis, F. Bordoni, A. Patyuchenko, and A. Moreira, "Advanced Concepts for Ultra-Wide-Swath SAR Imaging," in *European Conference on Synthetic Aperture Radar (EUSAR)*, vol. 2, Jun 2008, pp. 31–34.
- [5] G. Krieger, I. Hajnsek, K. Papathanassiou, M. Eineder, M. Younis, F. DeZan, P. Lopez-Dekker, S. Huber, M. Werner, P. Prats, H. Fiedler, R. Werninghaus, A. Freeman, P. Rosen, S. Hensley, B. Grafmüller, R. Bamler, and A. Moreira, "Tandem-L: A Mission for Monitoring Earth System Dynamics with High Resolution SAR Interferometry," in *8th European Conference on Synthetic Aperture Radar (EUSAR)*, Jun 2010, pp. 506–509.
- [6] A. Moreira, G. Krieger, I. Hajnsek, K. Papathanassiou, M. Younis, P. Lopez-Dekker, S. Huber, M. Villano, M. Pardini, M. Eineder, F. D. Zan, and A. Parizzi, "Tandem-L: A Highly Innovative Bistatic SAR Mission for Global Observation of Dynamic Processes on the Earth's Surface," *IEEE Geoscience and Remote Sensing Magazine*, vol. 3, no. 2, pp. 8–23, Jun 2015.
- [7] P. Rosen, Y. Kim, H. Eisen, S. Shaffer, L. Veilleux, S. Hensley, M. Chakraborty, T. Misra, R. Satish, D. Putrevu, and R. Bhan, "A dual-frequency Spaceborne SAR Mission Concept," in *IEEE International Geoscience and Remote Sensing Symposium (IGARSS)*, Jul 2013, pp. 2293–2296.
- [8] M. Villano, G. Krieger, and A. Moreira, "Staggered SAR: High-Resolution Wide-Swath Imaging by Continuous PRI Variation," *IEEE Transactions on Geoscience and Remote Sensing*, vol. 52, no. 7, pp. 4462–4479, Jul 2014.
- [9] —, "Data Volume Reduction in High-Resolution Wide-Swath SAR Systems," in *IEEE 5th Asia-Pacific Conference on Synthetic Aperture Radar (APSAR)*, Sep 2015, pp. 119–124.
- [10] P. Xaypraseuth, R. Satish, and A. Chatterjee, "NISAR Spacecraft Concept Overview: Design challenges for a proposed flagship dual-frequency SAR Mission," in *IEEE Aerospace Conference*, Mar 2014, pp. 1–11.
- [11] M. Younis, S. Huber, A. Patyuchenko, F. Bordoni, and G. Krieger, "Performance Comparison of Reflector- and Planar-Antenna based Digital Beam-Forming SAR," *International Journal of Antennas and Propagation*, vol. 2009, pp. 1–14, Jun 2009.